Journal of Visualized Experiments

Radiation treatment of organotypic cultures from submandibular and parotid salivary glands models key in vivo characteristics

--Manuscript Draft--

Article Type:	Methods Article - JoVE Produced Video
Manuscript Number:	JoVE59484R2
Full Title:	Radiation treatment of organotypic cultures from submandibular and parotid salivary glands models key in vivo characteristics
Keywords:	Submandibular salivary gland; vibratome culture; radiation; parotid salivary gland; organotypic culture; xerostomia
Corresponding Author:	Kirsten Limesand UNITED STATES
Corresponding Author's Institution:	
Corresponding Author E-Mail:	limesank@u.arizona.edu
Order of Authors:	Rachel Meyer
	Wen Yu Wong
	Roberto Guzman
	Randy Burd
	Kirsten Limesand
Additional Information:	
Question	**Response**
Please indicate whether this article will be Standard Access or Open Access.	Standard Access (US$2,400)
Please indicate the **city, state/province, and country** where this article will be **filmed**. Please do not use abbreviations.	Tucson, AZ USA

TITLE:

Radiation Treatment of Organotypic Cultures from Submandibular and Parotid Salivary Glands Models Key In vivo Characteristics

AUTHORS & AFFILIATIONS:

Rachel Meyer[1], Wen Yu Wong[2], Roberto Guzman[3], Randy Burd[1], Kirsten Limesand[1,2]

[1]Department of Nutritional Sciences, University of Arizona, Tucson, AZ, USA
[2]Cancer Biology Graduate Interdisciplinary Program, University of Arizona, Tucson, AZ, USA
[3]Department of Chemical Engineering, University of Arizona, Tucson, AZ, USA

Corresponding Author:

Kirsten Limesand (limesank@email.arizona.edu)

Email Addresses of Co-Authors:

Rachel Meyer (rachelmeyer@email.arizona.edu)
Wen Yu Wong (wwong3@email.arizona.edu)
Roberto Guzman (guzmanr@email.arizona.edu)
Randy Burd (rburd@email.arizona.edu)

KEYWORDS:

submandibular salivary gland, vibratome culture, radiation, parotid salivary gland, organotypic culture, xerostomia

SUMMARY:

Using three-dimensional organotypic cultures to visualize morphology and functional markers of salivary glands may provide novel insights into the mechanisms of tissue damage following radiation. Described here is a protocol to section, culture, irradiate, stain, and image 50–90 µm thick salivary gland sections prior to and following exposure to ionizing radiation.

ABSTRACT:

Hyposalivation and xerostomia create chronic oral complications that decrease the quality of life in head and neck cancer patients who are treated with radiotherapy. Experimental approaches to understanding mechanisms of salivary gland dysfunction and restoration have focused on in vivo models, which are handicapped by an inability to systematically screen therapeutic candidates and efficiencies in transfection capability to manipulate specific genes. The purpose of this salivary gland organotypic culture protocol is to evaluate maximal time of culture viability and characterize cellular changes following ex vivo radiation treatment. We utilized immunofluorescent staining and confocal microscopy to determine when specific cell populations and markers are present during a 30-day culture period. In addition, cellular markers previously reported in in vivo radiation models are evaluated in cultures that are irradiated ex vivo. Moving forward, this method is an attractive platform for rapid ex vivo assessment of murine and human salivary gland tissue responses to therapeutic agents that improve salivary function.

INTRODUCTION:

Proper salivary gland function is essential to oral health and is altered following head and neck cancer treatment with radiotherapy[1]. In 2017, nearly 50,000 new cases of head and neck cancer were reported in the United States[2]. Due to the tissue-damaging and frequently irreversible effects of radiation therapy on surrounding normal tissues such as salivary glands, patients are often left with severe side effects and diminished quality of life[2-4]. Common complications caused by radiation damage manifests in symptoms such as xerostomia (the subjective feeling of dry mouth), dental caries, impaired ability to chew and swallow, speech impairments, and compromised oral microbiomes[2-4]. These symptoms collectively can lead to malnutrition and impaired survival in affected individuals[5]. While salivary gland dysfunction in this population has been well-documented, the underlying mechanisms of damage to acinar cells have been disputed, and there is little integration among different animal models[6,7].

The current methods of studying salivary gland function and radiation-induced damage include the use of in vivo models, immortalized cell lines, two-dimensional (2-D) primary cell cultures, and three-dimensional (3-D) salisphere cultures[8-12]. Traditionally, cell culture models from immortalized cell lines and 2-D cultures involve single layered cells cultured on flat surfaces and are valuable for fast, easy, and cost-effective experimentation. However, artificial cell culture conditions can alter the differentiation status and physiological responses of cells exposed to various conditions, and the results often fail to translate to whole organism models[14,15]. In addition, immortalized cell cultures require modulation of p53 activity, which is critical for the salivary gland response to DNA damage[16,17].

3-D salisphere cultures are enriched for stem and progenitor cells at early time points in culture and have been useful for understanding the radiosensitivity of this subset of salivary gland cells[9,18]. A critical limitation of all these culture models is they are ineffective in visualizing the 3-D structure of the salivary gland, including the extracellular matrix (ECM) and cell-cell interactions over various layers, which are crucial in modulating salivary secretion[15]. The need for a method that encompasses the behavior of the tissue as a whole but can also be manipulated under laboratory conditions to study the effects of treatment is necessary to further discover the underlying mechanisms of radiation-induced salivary gland dysfunction.

Live tissue sectioning and culture has been documented previously[19,20] and is often used to study brain-tissue interactions[21]. In previous studies, parotid (PAR) salivary gland tissue from mice was sectioned at approximately 50 µm and cultured for up to 48 h, and analysis of viability, cell death, and function was performed thereafter[19]. Su et al. (2016) expanded on this methodology by culturing human submandibular glands (SMGs) sectioned at 35 µm or 50 µm for 14 days[20]. The proposed method is an advancement in that it includes both parotid and submandibular salivary glands sectioned at 50 µm and 90 µm and evaluation of the cultures for 30 days. The ability to cut a range of tissue thickness is important in evaluating cell-cell and cell-ECM interactions that are relevant for cellular processes including apical-basolateral polarity and innervation for secretion. Furthermore, the salivary gland slices were irradiated while in culture to determine the feasibility of this culture model to study radiation-induced salivary gland damage.

The purpose of this salivary gland organotypic culture protocol is to evaluate maximal time of culture viability and characterize cellular changes following ex vivo radiation treatment. To determine the maximum time sections that are viable post-dissection, trypan blue staining, live cell staining, and immunohistochemical staining for cell death were performed. Confocal microscopy and immunofluorescent staining were utilized to evaluate specific cell populations, morphological structures, and levels of proliferation. Tissue section cultures were also exposed to ionizing radiation to determine the effects of radiation on various markers in this 3-D model. Induction of cell death, cytoskeletal disruption, loss of differentiation markers, and compensatory proliferation in irradiated ex vivo cultures were compared to previous studies of in vivo models. This methodology provides a means to investigate the role of cell-cell interactions following radiation damage and provides an experimental model to efficiently evaluate the efficacy of therapeutic interventions (gene manipulations or pharmacological agents) that may be less suitable for in vivo models.

PROTOCOL:

1. **Preparation of vibratome**

1.1. Spray detachable components of the vibratome including the buffer tray, blade attachment, agarose block mold, and laboratory film with 70% ethanol, then UV-sterilize for at least 30 min.

1.2. Place and secure an additional sheet of laboratory film over the buffer tray to prevent ice from falling in.

1.3. Fill the ice chamber with crushed ice, remove the laboratory film from the buffer tray, and fill the buffer tray with 100 mL of ice-cold 1x phosphate buffered saline (PBS) solution supplemented with 1% penicillin-streptomycin-ampicillin (PSA).

1.4. Place a stainless steel razor blade into the blade holder. Use the screwdriver to tighten/loosen and change the angle of the blade.

2. **Preparation of tissue sample in agarose block and sectioning using the vibratome**

2.1. Autoclave all necessary dissection and sectioning tools including forceps, scissors, and paintbrushes.

2.2. Prepare 3% low melting point agarose in sterile 1x PBS and microwave until the agarose dissolves into solution. Ensure that the solution does not boil over and swirl the bottle periodically to mix.

NOTE: Prevent the low-melting agarose from solidifying by keeping it in a warm water bath. The low-melt agarose is fluid at 37 °C and sets at 25 °C. However, the water bath should be below 40

°C in order to pour the agarose around the tissue at physiological temperature.

2.3. Isolate salivary glands and place dissected tissue into 2 mL ice-cold 1x PBS supplemented with 1% PSA in a sterile, 30 mm culture dish.

2.4. Using autoclaved forceps, remove salivary glands from 1x PBS + 1% PSA solution and position at the bottom of an embedding mold. Fill the mold with liquid 3% low melting point agarose to cover the tissue.

2.5. Using the forceps, adjust the tissue to the middle of the block and position the salivary gland in the appropriate plane. The best cross sections for the submandibular and parotid glands are in the vertical plane.

2.6. Place agarose block on ice for 10 min to harden.

2.7. Carefully run a razor blade around the outer edge of the agarose to loosen and let the block slide out onto the UV-sterilized laboratory film from step 1.1.

2.8. Use a razor blade to cut out an agarose box containing the salivary gland. Ensure that the plane of section is straight and parallel to the opposite side of the block (the surface that will be glued down). Since the agarose does not infiltrate the tissue, do not trim off too much agarose around the tissue so the tissue will be well supported.

2.9. Use superglue to attach the block to the cutting surface.

2.10. Section at 50 µm or 90 µm thickness by vibratome at a speed of 0.075 mm/s and frequency of 100 Hz.

NOTE: Setting the vibratome at the highest frequency and lowest blade speed provides the most optimal slices.

2.11. Collect sections in a 24-well tissue culture dish containing ~1 mL ice-cold PBS per well using an autoclaved, natural hair paintbrush, placing the brush in 70% ethanol between slice collections to maintain sterility.

3. **Culturing sections**

3.1. Autoclave a micro-spatula and forceps.

3.2. Make stock vibratome culture media with or without fetal bovine serum (FBS): DMEM/F12 media supplemented with 1% PSA, 5 µg/mL transferrin, 1.1 µM hydrocortisone, 0.1 µM retinoic acid, 5 µg/mL insulin, 80 ng/mL epidermal growth factor, 5 mM L-glutamine, 50 µg/mL gentamicin sulfate, and 10 µL/mL trace element mixture. Add an appropriate amount of FBS to make 0%, 2.5%, 5.0%, or 10% solutions.

3.3. Prior to sectioning, add 300 µL of pre-warmed media and place a 12 mm diameter, 0.4 µm pore-size membrane insert into each well of a 24-well tissue culture plate. The media should reach the membrane bottom to create a liquid-air interface for culture.

3.4. Gently lay the salivary sections on top of the membrane insert using the micro spatula and culture at 37 °C in humidified 5% CO_2 and 95% air atmosphere incubator.

3.4.1. Add approximately 300 µL primary culture media into the well and a few drops into the membrane inserts (approximately 40 µL) every other day or as needed. Proper culturing showed that the cells are able to survive and be maintained for up to 30 days ex vivo.

4. Irradiation of salivary gland sections

4.1. Treat sections with a single dose of radiation (5 Gy) using cobalt-60 (or equivalent) irradiator.

4.1.1. Transport sections to irradiator facility using a covered styrofoam container to avoid fluctuations in temperature. In addition, care needs to be taken during transport back to the laboratory incubator to ensure that media does not splash onto culture lid and induce contamination.

4.1.2. Place the 24-well plate containing salivary gland sections 80 cm from the radiation source, in the center of a 32" x 32" radiation field. Radiation dose calculations and corresponding time in irradiator will vary by instrument and cobalt-60 decay.

4.2. Continue monitoring and culturing these sections as described in section 3.

5. Viability staining

5.1. Aspirate old media and wash slices twice with sterile, pre-warmed 1x PBS.

5.2. Stain sections with trypan blue dye.

5.2.1. Use a micro-spatula to move the slice from the culture to a glass slide.

5.2.2. Add 0.4% trypan blue solution to the vibratome slice with enough volume to cover the tissue (10–20 µL).

5.2.3. Incubate slices at room temperature (RT) in the trypan blue for 1–2 min for the dye to penetrate the tissue. Nonviable cells will be stained blue, and viable cells will be unstained.

5.3. Stain sections with calcein, AM live-cell dye.

5.3.1. Add enough volume of stain to cover the section in one well of a 24 well-plate (200–300 µL).

5.3.2. Incubate slices at RT for 15 min to allow dye penetration.

5.3.3. Carefully remove the section from the well and place on a glass slide. Mount slices with 1 drop of mounting media.

5.3.4. Image sections on a fluorescent microscope at excitation/emission wavelengths of 488 nm and 515 nm.

6. **Antibody staining vibratome sections**

NOTE: The following provides a general antibody staining protocol specific for Ki-67; however, this protocol can be used with any antibody. All washes are conducted at RT unless otherwise noted.

6.1. In the multi-well tissue culture dish, aspirate off media and wash at least 2x with sterile 1x PBS.

6.2. Fix sections using 4% paraformaldehyde (PFA) overnight at 4 °C.

6.3. Aspirate off 4% PFA and wash 3x with PBT [1x PBS, 1% bovine serum albumin (BSA), 0.1% Triton X-100].

NOTE: Sections can be stored in 1x PBS at 4 °C and stained at a later time. Maximum storage time tested in this manuscript was 3 weeks. Longer storage time will need to be optimized by the individual user if that is desired.

6.4. Permeabilize sections using 0.3% Triton X-100 in 1x PBS for 30 min.

NOTE: This step can be modified and optimized for specific antibody staining and permeabilization.

6.5. Pipet off permeabilization solution.

6.6. Wash slices 3x for 5 min with 1x PBS, 1% BSA, and 0.1% Triton X-100 (PBT).

6.7. Block the slices with blocking agent with 1% normal goat serum for 1 h.

6.8. Wash the slices 3x for 5 min with PBT.

6.9. Incubate the slices overnight at 4 °C with 500 µL anti-Ki67 rabbit monoclonal antibody diluted in 1% BSA in 1x PBS.

NOTE: For phalloidin staining, skip step 6.9 and proceed using the protocol for the specific phalloidin used. For DNA counterstain, skip to step 6.15.

6.10. Aspirate anti-Ki67 rabbit monoclonal antibody.

6.11. Wash the slices 6x for 5 min in 1x PBS.

6.12. Incubate the slices in 500 µL of fluorescently conjugated secondary antibody compatible with the anti-Ki67 antibody diluted in 1% BSA in 1x PBS at RT for 1.5 h covered from light.

NOTE: Based on secondary antibody used, incubation time with the secondary antibody can be further optimized by the individual user. In addition, the secondary antibody is light-sensitive. All subsequent washes must be performed in the dark.

6.13. Aspirate secondary antibody.

6.14. Wash slices for 3x for 5 min with 1x PBS.

6.15. Wash slices for 5 min in deionized water.

6.16. Counterstain slices with DAPI (1µg/mL) for 20 min at RT.

6.17. Wash slices (once) for 5 min in deionized water.

6.18. Mount slices with one drop (~40 µL) of mounting media. To avoid excess bubbles, slowly place the coverslip onto the mounting media on the slide, starting with a 45° angle.

6.18.1. To prevent crushing the thick sections with the coverslip, mount each slice with a spacer. A spacer can be created by placing a rim of vacuum grease in a square around the tissue section.

6.18.2. When laying the coverslip, the edges of the coverslip can be sealed with vacuum grease. Press down on the edges of the coverslip with your thumb to firmly adhere it onto the slide. Alternatively, seal the coverslip onto the microscope slide using clear nail polish.

7. **Imaging vibratome sections**

7.1. Image the stained slides within 5 days of staining.

7.2. Obtain optical sections of the stained vibratome slices using a confocal microscope. With a confocal microscope, obtain a z-stack at a defined step size or take individual images depending on the user's experimental design. Images can be examined on any computer screen after confocal collection.

NOTE: Due to the thickness of the vibratome slices, it is recommended that a confocal microscope or a scope with z-stack capability is used to visualize details within the samples. For the images used in this manuscript, a 63x oil objective was used; however, this can be tailored and further modified by the individual user and the specific scope used. Recommended pixel resolution for each objective and zoom factor with the assumed Nyquist sampling of 2.5 pixels in X and Y for the smallest optically resolvable structure was used. However, some commentators suggest 2.3 pixels, while others suggest 2.8 pixels. Please refer to the Handbook of Biological Confocal Microscopy[22] for further details on how to make these calculations.

REPRESENTATIVE RESULTS:

Primary 2-D cultures are grown in fetal bovine serum (FBS) supplemented media while primary 3-D salisphere culture are typically cultured in serum-free conditions[10,11]. In addition, the two previous studies utilizing vibratome cultures from salivary glands cultured their sections in 0% or 10% FBS supplemented media[19,20]. Mouse submandibular slices were sectioned at a thickness of 50 µm using a vibratome and optimal culture conditions were determined using a series of FBS concentrations (0%, 2.5%, 5.0%, and 10%). To determine survival characteristics, bright-field microscope images were taken at culture days 1, 4, 7, 14 ,and 30 post-sectioning (**Figure 1**). Additionally, gland sections were stained with 0.4% trypan blue dye and imaged with a bright-field microscope at 40x at the indicated time points (**Figure 2A**). Non-viable cells were stained blue and viable cells remained clear.

Similarly, to determine the survival characteristics of thicker slices sectioned at 90 µm, bright-field microscope images with and without trypan blue staining were taken at day 30 in cultures supplemented with 2.5% FBS (**Figure 2B**). Due to the slice thickness, 90 µm sections stained with trypan blue dye were imaged whole then cut in half in order to evaluate the center of the slice (**Figure 2B**). As a confirmation, a live-cell dye was utilized to evaluate cell survival in different FBS culturing conditions (**Figure 2C**). In bright-field images, high levels of translucent, surviving cells in tissues sectioned at both 50 µm and 90 µm were observed. Interestingly, sections became darker and overall tissue area condenses over time in culture, yet a significant portion of the section appears to survive the 30-day culture period (**Figure 1, Figure 2**). This condensation was most evident in the 0% and 10% FBS culturing conditions. Trypan blue positive cells were observed on the perimeter of all sections regardless of culturing conditions, and there was an increase in trypan blue positive cell area in 0% FBS culture conditions when compared to the higher FBS culturing conditions (**Figure 2A,2B**).

Using the live cell stain, the sections cultured in 0% showed the lowest amount of staining, and the addition of FBS to the culture media improved the amount of live cells. Taken together, sections cultured in 0% FBS showed visible tissue condensation, elevated trypan blue stained areas, and the lowest levels of live cell staining. The addition of 2.5% FBS to the cultures improved the amount of translucent tissue, decreased the trypan blue positive area, and increased the levels of live cell staining. Additional increases in FBS concentration did not appear to improve survivability of the tissue; therefore, 2.5% FBS in the vibratome media was the optimal FBS concentration and utilized as the culture condition for all subsequent experiments.

To determine the viability of the submandibular ex vivo tissue slices post-dissection, proliferative and apoptotic markers were evaluated at days 1, 3, 7, 14, and 30 in culture. The proliferative activity was assessed by Ki67 immunostaining in a subset of culture slices (**Figure 3A**). Ki67 positive cells were observed at all time points evaluated and continued to be present at day 30 in culture, with minimal differences between time points. Similarly, the degree of apoptosis was evaluated by cleaved caspase-3 immunostaining in a separate subset of sections (**Figure 3B**). A low level of cleaved caspase-3 positive cells was observed at all time points up to day 14 in culture, while day 30 conditions appeared to have a small increase in the number of cleaved caspase-3 positive cells in some areas. Evaluation of the tissue edges did not reveal higher levels of cleaved caspase-3, which does not recapitulate the trypan blue staining (**Figure 2**). Overall, these results suggest that cues for proliferation and viability remained present in the vibratome cultures during the 30-day evaluation period.

Thick section vibratome cultures allow the opportunity to evaluate interactions between cellular constituents of a particular tissue at a depth that includes more than one epithelial cell thickness in each direction. In addition, it is important to be able to culture both major salivary glands, as they differ in the composition of salivary proteins produced, histological architecture, radiosensitivity, and other critical features. To determine different cellular populations in submandibular gland cultures, submandibular sections were stained with E-cadherin (E-cad) to detect epithelial cells, smooth muscle actin (SMA) to detect myoepithelial cells, and actin filaments (phalloidin) to detect cytoskeletal structures during the 30 days in culture (**Figure 4A**).

E-cadherin staining was observed on the membranes of a majority of cells and detected throughout the 30-day culture period. SMA+ cells were detected throughout the culture period, with similar levels at each time point. Cytoskeletal organization of actin filaments also appeared to be maintained at each time point evaluated. In contrast, there were cellular markers that were not consistently maintained during the entire evaluation period and these included CD31 (vasculature), TUBB3 (neurons), and Aquaporin-5 (Aqp-5, acinar marker) (**Figure 4B**). Vascular structures through the confocal stacks were clearly observed at days 1 and 3 post-culture; however, these structures appeared fragmented at day 7. Similarly, neuronal processes were intact during the first day of culture, appeared diminished at day 3, and were subsequently lost at day 7 in culture. Aqp5+ cells were observed at days 1, 3, 7, and 14 in culture; albeit, at day 14, the overall staining level appeared to be reduced, with a more granular resemblance in the remaining positive cells. These data suggest that submandibular cultures contain the diversity of tissue constituents with maintenance of the vascular and neuronal cell types for shorter culture periods, and epithelial and myoepithelial cell types for longer culture periods.

While vibratome-sectioned cultures have been previously reported for the parotid salivary gland, the cultures were maintained for 48 h, limiting the timeframe during which they could be studied. In order to determine whether parotid glands can be maintained for longer, murine parotid glands were sectioned and cultured for 1, 3, 7, or 14 days. Fewer sections were obtained from the parotid gland due to its smaller size in mice; therefore, a 30-day culture period was not attempted. Slices were evaluated for proliferation by immunofluorescent staining using antibody against Ki67. Similar to the submandibular cultures, Ki67 positive cells were observed at all time

points, indicating that the cells are maintaining a degree of proliferation in culture (**Figure 5A**).

In addition, the maintenance of functional acinar markers (α-amylase and Aqp5), an epithelial marker (E-cad), and vascular (CD31) and neuronal (TUBB3) cell populations were evaluated. Amylase is one of the most abundant proteins produced by differentiated parotid epithelial cells and frequently lost during the 2-D culturing of primary parotid cells. In the vibratome cultures, amylase was observed in the acinar cells and excluded from the ductal cells throughout the 14-day culture period (**Figure 5B**). Similar to the submandibular cultures, Aqp5+ cells were present in the parotid cultures at each time point, with the day 14 cultures exhibiting reduced levels compared to earlier time points (**Figure 5C**). E-cadherin levels were also maintained on the membranes of a majority of cells during the 14-day culture period (**Figure 5D**). Neuronal structures appeared to be maintained during the 7 day culture period and were not assessed at later time points (**Figure 5E**). In contrast, vascular structures appeared intact during the first day in culture, and only smaller structures were present at days 3 and 7 in culture (**Figure 5F**). These data suggest that parotid cultures maintain their proliferative capabilities and most functional capabilities for 7-14 days in culture and potentially exhibit a more intact tissue structure for a longer time frame.

The functional utility of the vibratome culture model was addressed by treating parotid or submandibular cultures with a single dose of radiation (**Figures 6, Figure 7, Figure 8**). Previous work in irradiated mouse models has focused on the parotid gland and demonstrated the induction of apoptosis that peaks at 24 h, induction of compensatory proliferation starting at day 5, disruption of actin filaments starting at day 5, and loss of differentiation markers (e.g., amylase) by day 14[23,24,26]. Irradiation of parotid vibratome cultures led to increases in apoptosis at day 1, increases in proliferation at day 7, disruption of actin filaments at day 7, and reductions in amylase at day 7 (**Figure 6**). Irradiation of submandibular vibratome cultures led to increases in apoptosis at days 1 and 3, increases in proliferation at day 7, and disruption of actin filaments at day 7 (**Figure 7**). E-cadherin levels appeared relatively intact in both parotid and submandibular cultures, which was similar to in vivo observations[26]. The functional acinar cell markers Aqp-5 in submandibular gland sections and amylase in parotid gland sections decreased at day 14, compared to corresponding untreated time points (**Figure 8**). These data suggest that radiation-induced tissue changes that were observed in vivo were also observed in irradiated vibratome cultures.

FIGURE AND TABLE LEGENDS:

Figure 1: Bright-field microscope images of 50 µm submandibular sections. Submandibular glands from female FVB mice (4-8 weeks old) were dissected, sectioned to 50 µm thickness, and cultured on organotypic cell culture inserts for 1, 4, 7, 14, and 30 days post-dissection at 0%, 2.5%, 5.0%, and 10% fetal bovine serum (FBS) in media to determine culture characteristics and optimize culture conditions. Scale bars = 200 µm.

Figure 2: Viability staining of submandibular sections. (**A)** Bright-field microscope images of 50 µm submandibular dissected from 4- to 8-week old female FBV mice and stained with trypan blue (0.4%) at 1, 3, 7, 14, and 30 days in culture with media containing 2.5% fetal bovine serum (FBS).

(**B)** Bright-field microscope images of 90 µm submandibular sections (left panel), stained with trypan blue (middle panel), cut in half and stained with trypan blue (right panel), then cultured to 30 days post-dissection in media containing 2.5% FBS. **(C)** Fluorescent images of 50 µm submandibular sections cultured in various FBS concentrations (0%, 2.5%, 5%, 10%) stained with calcein AM to indicate live cells (green) at culture day 7. Scale bars = 200 µm.

Figure 3: Evaluation of proliferative and apoptotic markers in submandibular organotypic tissue slices. Submandibular glands from female FVB mice (4-8 weeks old) were dissected, sliced to 50 µm thickness, and cultured in media supplemented with 2.5% FBS on organotypic cell culture inserts for 1, 3, 7, 14, and 30 days post-dissection. At the indicated time points, slices were fixed and stained for proliferative (Ki67) and apoptotic (cleaved caspase-3) markers. (**A)** Immunofluorescent staining of Ki67-positive cells (green) and the nucleus (blue). (**B)** Immunofluorescent staining of cleaved caspase-3-postive cells (red) and the nucleus (blue) from two viewpoints of a slice. The top row panel displays cleaved caspase-3-positive cells on the edge of a slice, and the bottom row panel displays cleaved caspase-3-positive cells from the middle of a slice. Representative confocal images were selected from multiple z-stacks per time point. Scale bars = 30 µm.

Figure 4: Presence of cellular structures in submandibular organotypic tissue slices. Submandibular glands from female FVB mice (4-8 weeks old) were dissected, sliced to 50 µm thickness, and cultured in media supplemented with 2.5% FBS on organotypic cell culture inserts for 1, 3, 7, 14, or 30 days post-dissection. At the indicated time points, slices were fixed and stained for their corresponding markers with the nucleus (blue). **(A)** Submandibular sections were evaluated at days 1, 7, 14, and 30 post-dissection for the levels of E-cadherin, smooth muscle actin (SMA), and F-actin (phalloidin). **(B)** Submandibular sections were evaluated at days 1, 3, and 7 for levels of CD31 (vasculature) and TUBB3 (neurons). Aquaporin-5 (Aqp5) was evaluated at days 1, 3, 7, and 14. Representative confocal images were selected from multiple z-stacks per time point. Scale bars = 30 µm.

Figure 5: Evaluation of proliferative and functional markers in PAR organotypic tissue slices. Parotid glands from female FVB mice (4-8 weeks old) were dissected, sliced to 50 µm thickness, and cultured in media supplemented with 2.5% FBS on organotypic cell culture inserts for 1, 3, 7, or 14 days post-dissection. At the indicated time points, slices were fixed and stained for their corresponding markers with the nucleus (blue). **(A)** Immunofluorescent staining of Ki67-positive cells (green). **(B)** Immunofluorescent staining of amylase-positive cells (red). **(C)** Immunofluorescent staining of aquaporin-5 (Aqp5)-positive cells (green). **(D)** Immunofluorescent staining of E-cadherin (red) positive cells. **(E)** Immunofluorescent staining of neurons indicated by TUBB3 (magneta) positive cells. **(F)** Immunofluorescent staining of the vasculature indicated by CD31 (red) positive cells. Representative confocal images were selected from multiple z-stacks per time point. Scale bars = 30 µm; d = ductal cells.

Figure 6: Cellular changes following irradiation of parotid organotypic tissue slices. Parotid glands from female FVB mice (4-8 weeks old) were dissected, sliced to 50 µm thickness, and cultured in supplemented with 2.5% FBS on organotypic cell culture inserts. On day 1 post-

dissection, a subset of slices was exposed to 5 Gy radiation and maintained for 2, 4, or 8 days post-dissection (corresponds to days 1, 3, and 7 post-radiation). Immunofluorescent staining of untreated and irradiated parotid sections to determine levels of **(A)** Ki67 (green)-positive cells, **(B)** cleaved caspase 3 (red)-positive cells, **(C)** phalloidin (cyan)- positive cells, **(D)** amylase (red)-positive cells, and **(E)** E-cadherin (red) positive cells. All nuclear staining utilized DAPI (blue). Representative confocal images were selected from multiple z-stack per time point. Scale bars = 30 µm.

Figure 7: Cellular changes following irradiation of submandibular organotypic tissue slices. Submandibular glands from female FVB mice (4-8 weeks old) were dissected, sliced to 50 µm thickness, and cultured in media supplemented with 2.5% FBS on organotypic cell culture inserts. On day 1 post-dissection, a subset of slices was irradiated with 5Gy and maintained for 2, 4, or 8 days post-dissection (corresponds to days 1, 3, and 7 post-radiation). Immunofluorescent staining of untreated and irradiated submandibular sections to determine levels of **(A)** Ki67 (green)-positive cells, **(B)** cleaved caspase 3 (red)-positive cells, **(C)** phalloidin (cyan)- positive cells, **(D)** aquaporin 5 (Aqp5) (green)-positive cells, and **(E)** E-cadherin (red) positive cells. All nuclear staining utilized DAPI (blue). Representative confocal images were selected from multiple z-stack per time point. Scale bars = 30 µm.

Figure 8: Functional acinar markers in irradiated parotid and submandibular organotypic tissue slices. Submandibular and parotid glands from female FVB mice (4-8 weeks old) were dissected, sliced to 50 µm thickness, and cultured in media supplemented with 2.5% FBS on organotypic cell culture inserts. On day 1 post-dissection, a subset of slices was irradiated with 5Gy and maintained for 14 days post-irradiation. Immunofluorescent staining of untreated (UT) and irradiated (IR) sections were used to determine levels of **(A)** aquaporin-5 (Aqp5) (green)-positive cells and **(B)** amylase (red)-positive) cells. All nuclear staining utilized DAPI (blue). Representative confocal images were selected from multiple z-stack per time point. Scale bars = 30 µm.

DISCUSSION:

Salivary gland research has utilized a number of culture models, including immortalized 2-D cultures, primary 2-D cultures, 3-D salisphere cultures, and 3-D organ cultures from embryonic explants to ascertain questions on underlying biology and physiology. These culture models have yielded insightful information across a diverse array of research questions and will continue to be important tools in salivary research. The limitations of these culture models include modulation of p53 activity during immortalization, transient viability of primary cultures, loss of differentiation and secretory proteins in culture, and inability to evaluate cell-cell, cell-ECM and polarity interactions in adult tissues. The first 3-D organotypic slice culture (vibratome sectioned cultures) method for salivary glands was published in 2008[18]; however, this technique has been largely underutilized in this field despite frequent use in other fields. The work cultured parotid sections for 48 h, which limits the ability to study these sections for chronic effects following radiation treatment or utilize transfection or transduction protocols for phenotypes following manipulation of specific genes. The method described here has been optimized to allow for longer time in culture, yield high resolution images through confocal microscopy, provide a

method to study intra- and intercellular dynamics on a 3-D section, and evaluate radiation-induced changes during a culture period of at least 14 days.

While each step is required for implementation of the technique, some steps are crucial to successful sectioning and culture maintenance. These include cutting the salivary gland slices, maintaining the slices in culture, and staining and imaging the slices with confocal microscopy. The presented protocol poses some challenges that require patience and practice in order to obtain optimal slices for analysis. The following suggestions will assist in carrying out this protocol successfully. It is imperative to completely isolate the salivary gland from the surrounding connective tissue following dissection. Residual connective tissue causes the vibratome blade to drag the gland out from the agarose block and requires the tissue to be re-embedded in agarose. This can be a major limitation since multiple re-embedding can increase the chances of contamination and decrease the viability of the slices. This is especially crucial for culturing parotid glands, since the parotid glands are more lobular in structure and therefore more likely to have extraneous tissue.

The addition of 1% penicillin-streptomycin-amphotericin B (PSA) to all liquids including the buffer tray, the slice collection dish, and the vibratome media minimizes contamination of the slices post-dissection. Variation of agarose concentration was used to optimize successful cutting. Due to the density of the salivary glands, 1.9% agarose was too soft, and the glands were easily dislodged from the block. Vibratome sectioning in other fields have used 5.0% agarose; however, this caused jagged cuts and slices were suboptimal. After testing several agarose percentage conditions, 3% agarose was the most optimal to support the weight and firmness of the tissue. Notably, the agarose concentration utilized in Warner et al. and Su et al. was also 3%[19,20].

Additionally, the angle, frequency of vibration, and advancing speed of the blade can be modified based on the tissue to be sectioned. For submandibular and parotid salivary glands, a 15° angle, speed of 0.075 mm/s, and frequency of 100 Hz were appropriate for sectioning. Due to the softness of the salivary glands, the optimal cutting conditions required the blade to advance slowly through the tissue at a high vibration. For immunofluorescent staining, the permeabilization, duration of incubations, and wash steps are essential for optimal stains. If positive staining only appears in the outer layers of the tissue slice, a more stringent permeabilization with proteinase K may be needed, while uneven staining or high background staining may require a less stringent staining with 0.2% Triton X-100. The incubation times were optimized for high signal and low background, which may need to be tailored to specific primary antibodies. Longer wash steps are essential in reducing high background and this may be tailored to the specific antibodies used.

One major application of this methodology is extended kinetic analysis following radiation exposure of salivary glands. Prior work has established both acute and chronic phase changes in irradiated salivary glands[6, 24-26], and the vibratome culture system can be a powerful tool to dissect out the critical molecular events at specific time points after treatment. For example, radiation-induced cellular changes in the salivary gland that have been reported in the literature, including reductions in amylase, apoptosis of acinar cells, compensatory proliferation of acinar

cells, loss of polarity and disruptions in cytoskeletal structure. Notably, vibratome cultures irradiated ex vivo exhibit similar alterations in these markers.

In addition, the acute phase response in salivary glands pivots around p53 activity; however, it is unclear what role p53 plays in later time points due to the ~5-day viability of primary cultures. This system would allow ex vivo, controlled disruption of p53 activity at later time points and uncover a role in chronic damage or regenerative responses. Furthermore, the compensatory proliferation response is initiated 5 days after radiation treatment, and it is difficult to delineate the molecular regulators of this response in transient primary cultures. The most widely used application of this methodology will likely involve cell-cell, cell-ECM, and polarity interactions in adult tissues. Impactful studies have been conducted in 3-D organ cultures from embryonic glands to uncover the intricate interaction between developing salivary glands and the neuronal or vascular network[27-31].

The method described here indicates that further optimization is needed for neuronal or vascular work in the submandibular cultures and possibly parotid cultures. Radiation damage also disrupts junctional regulators, induces collagen deposition, alters F-actin organization, and modulates secretory granules[26,30,32]. Salivary gland regeneration studies are handicapped by the absence of an adult model to evaluate these interactions. This organotypic culture method can provide a system to apply advanced molecular techniques and further study the regulation of these mediators in a 3-D context and efficiently discover new therapies.

ACKNOWLEDGMENTS:
This work was supported in part by pilot funding provided by University of Arizona Office of Research and Discovery and National Institutes of Health (R01 DE023534) to Kirsten Limesand. The Cancer Biology Training Grant, T32CA009213, provided stipend support for Wen Yu Wong. The authors would like to thank M. Rice for his valuable technical contribution.

DISCLOSURES:
The authors have nothing to disclose.

REFERENCES:
1. Dirix, P., Nuyts, S., Van den Bogaert, W. Radiation-induced xerostomia in patients with head and neck cancer: a literature review. *Cancer*. **107** (11), 2525-2534 (2006).
2. Siegel, R. L., Miller, K. D., Jemal, A. Cancer Statistics, 2017*. CA: A Cancer Journal for Clinicians.* **67** (1), 7-30 (2017).
3. Hancock, P. J., Epstein, J. B., Sadler, G. R. Oral and dental management related to radiation therapy for head and neck cancer. *Journal of the Canadian Dental Association.* **69** (9), 585-590 (2003).
4. Nguyen, N. P. et al. Quality of life following chemoradiation and postoperative radiation for locally advanced head and neck cancer. *Journal for Oto-rhino-laryngology and Its Related Specialties.* **69** (5), 271-276 (2007).
5. Gorenc, M., Kozjek, N. R., Strojan, P. Malnutrition and cachexia in patients with head and neck cancer treated with (chemo)radiotherapy. *Reports of Practical Oncology and Radiotherapy:*

Journal of Greatpoland Cancer Center in Poznań and Polish Society of Radiation Oncology. **20** (4), 249-258 (2015).

6. Grundmann, O., Mitchell, G. C., Limesand, K. H. Sensitivity of salivary glands to radiation: from animal models to therapies. *Journal of Dental Research*. **88** (10), 894-903 (2009).

7. Konings, A. W., Coppes, R. P., Vissink, A. On the mechanism of salivary gland radiosensitivity. *International Journal of Radiation Oncology, Biology, and Physics*. **62** (4), 1187-1194 (2005).

8. Chan, Y.-H., Huang, T.-W., Young, T.-H., Lou, P.-J. Human salivary gland acinar cells spontaneously form three-dimensional structures and change the protein expression patterns. *Journal of Cellular Physiology.* **226** (11), 3076–3085 (2011).

9. Nguyen, V. T., Dawson, P., Zhang, Q., Harris, Z., Limesand, K. H. Administration of growth factors promotes salisphere formation from irradiated parotid salivary glands. *PLoS ONE.* **13** (3), e0193942 (2018).

10. Limesand, K. H. et al. Characterization of Rat Parotid and Submandibular Acinar Cell Apoptosis In Primary Culture. *In Vitro Cellular & Developmental Biology - Animal* **39** (3), 170 (2003).

11. Wei, L., Xiong, H., Li, W., Li, B., Cheng, Y. Upregulation of IL-6 expression in human salivary gland cell line by IL-17 via activation of p38 MAPK, ERK, PI3K/Akt, and NF-κB pathways. *Journal of Oral Pathology & Medicine*. **47** (9), 847–855 (2018).

12. Chuong, C., Katz, J., Pauley, K. M., Bulosan, M., Cha, S. RAGE expression and NF-κB activation attenuated by extracellular domain of RAGE in human salivary gland cell line. *Journal of Cellular Physiology.* **221** (2), 430–434 (2009).

13. Edmondson, R., Broglie, J. J., Adcock, A. F., Yang, L. Three-dimensional cell culture systems and their applications in drug discovery and cell-based biosensors. *Assay and Drug Development Technologies.* **12** (4), 207-218 (2014).

14. Bhadriraju, K., Chen, C. S. Engineering cellular microenvironments to improve cell-based drug testing. *Drug Discovery Today.* **7** (11), 612-620 (2002).

15. Breslin, S., O'Driscoll, L. Three-dimensional cell culture: the missing link in drug discovery. *Drug Discovery Today*. **18** (5-6), 240-249 (2013).

16. Avila, J. L., Grundmann, O., Burd, R., Limesand, K. H. Radiation-induced salivary gland dysfunction results from p53-dependent apoptosis. *International Journal of Radiation Oncology, Biololgy, Physics.* **73** (2), 523-529 (2009).

17. Mitchell, G. C. et al. IGF1 activates cell cycle arrest following irradiation by reducing binding of DeltaNp63 to the p21 promoter. *Cell Death & Disease.* **1,** e50 (2010).

18. Lombaert, I. M. A. et al. Rescue of Salivary Gland Function after Stem Cell Transplantation in Irradiated Glands. *PLoS ONE.* **3** (4), (2008).

19. Warner, J. D. et al. Visualizing form and function in organotypic slices of the adult mouse parotid gland. *American Journal of Physiology-Gastrointestinal and Liver Physiology.* **295** (3), G629-640 (2008).

20. Su, X. et al. Three-dimensional organotypic culture of human salivary glands: the slice culture model. *Oral Diseases.* **22** (7), 639-648 (2016).

21. Mattei, G., Cristiani, I., Magliaro, C., Ahluwalia, A. Profile analysis of hepatic porcine and murine brain tissue slices obtained with a vibratome. *PeerJ - The Journal of Life and Environmental Sciences.* **3,** e932 (2015).

22. Pawley, J. ed. *Handbook of Biological Confocal Microscopy*. 3rd ed. Springer U.S. Boston, MA. (2006).
23. Limesand, K. H. et al. Insulin-Like Growth Factor–1 Preserves Salivary Gland Function After Fractionated Radiation. *International Journal of Radiation Oncology, Biology, and Physics.* **78**(2), 579–586 (2010).
24. Grundmann, O., Fillinger, J. L., Victory, K. R., Burd, R., Limesand, K. H. Restoration of radiation therapy-induced salivary gland dysfunction in mice by post therapy IGF-1 administration. *BMC Cancer.* **10,** 417 (2010).
25. Chibly, A. M. et al. aPKCzeta-dependent Repression of Yap is Necessary for Functional Restoration of Irradiated Salivary Glands with IGF-1. *Scientific Reports.* **8** (1), 6347 (2018).
26. Wong, W. Y., Pier, M., Limesand, K. H. Persistent disruption of lateral junctional complexes and actin cytoskeleton in parotid salivary glands following radiation treatment. *American Journal of Physiology: Regulatory, Integrative and Comparative Physiology.* **315** (4), R656-R667 (2018).
27. Emmerson, E. et al. SOX2 regulates acinar cell development in the salivary gland. *eLife.* **6**, (2017).
28. Nedvetsky, P. I. et al. Parasympathetic innervation regulates tubulogenesis in the developing salivary gland. *Developmental Cell.* **30** (4), 449-462 (2014).
29. Kwon, H. R., Nelson, D. A., DeSantis, K. A., Morrissey, J. M., Larsen, M. Endothelial cell regulation of salivary gland epithelial patterning. *Development.* **144** (2), 211-220 (2017).
30. Mellas, R. E., Leigh, N. J., Nelson, J. W., McCall, A. D., Baker, O. J. Zonula occludens-1, occludin and E-cadherin expression and organization in salivary glands with Sjogren's syndrome. *Jounral of Histochemistry and Cytochemistry.* **63** (1), 45-56 (2015).
31. Daley, W. P. et al. Btbd7 is essential for region-specific epithelial cell dynamics and branching morphogenesis in vivo. *Development.* **144** (12), 2200-2211 (2017).
32. Nam, K. et al. Post-Irradiated Human Submandibular Glands Display High Collagen Deposition, Disorganized Cell Junctions, and an Increased Number of Adipocytes. *Journal of Histochemistry and Cytochemistry.* **64** (6), 343-352 (2016).

Figure

Click here to access/download;Figure;FIG 1 comp.pdf

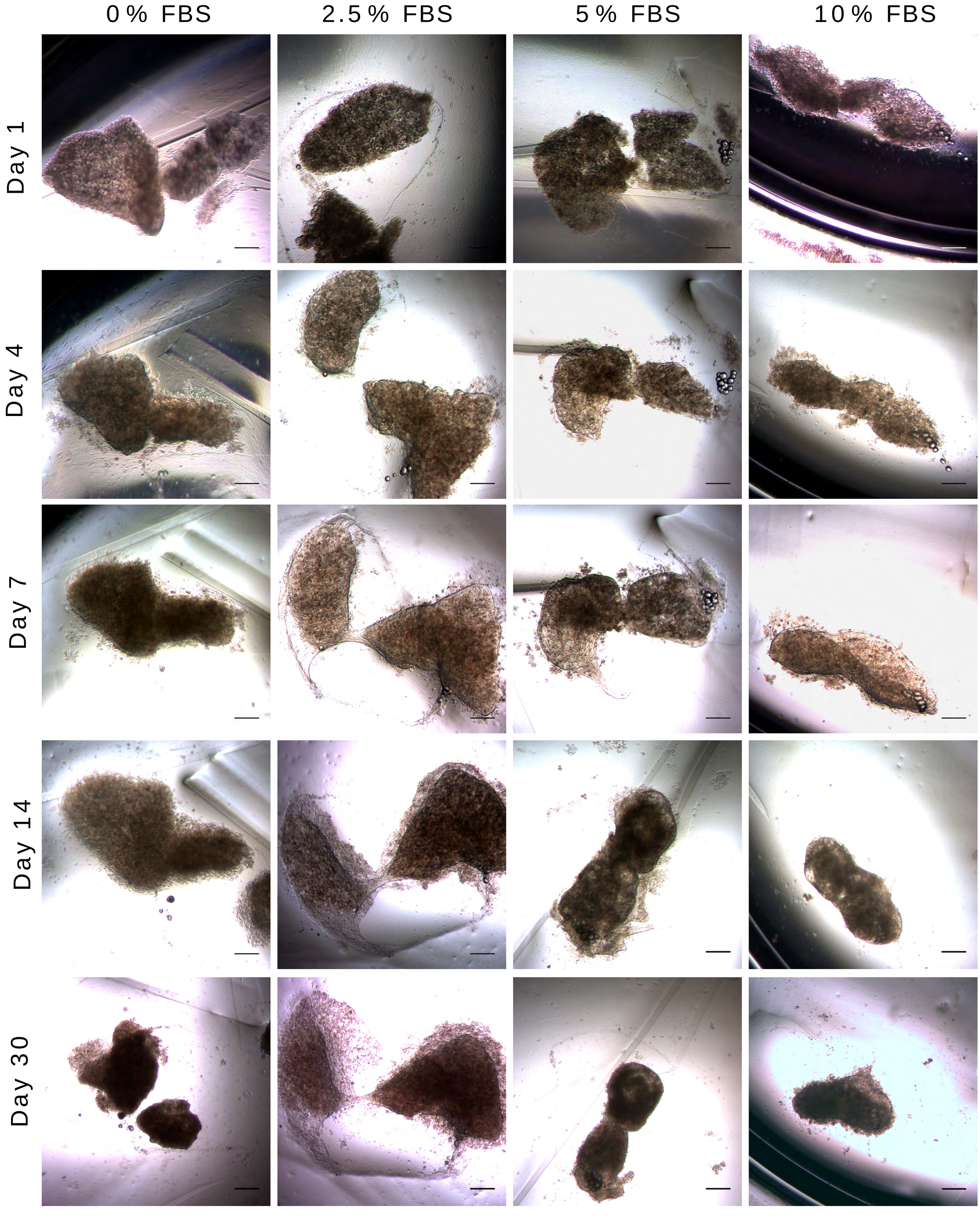

Figure

Click here to access/download;Figure;Fig 2 UPDATED JOVE.pdf

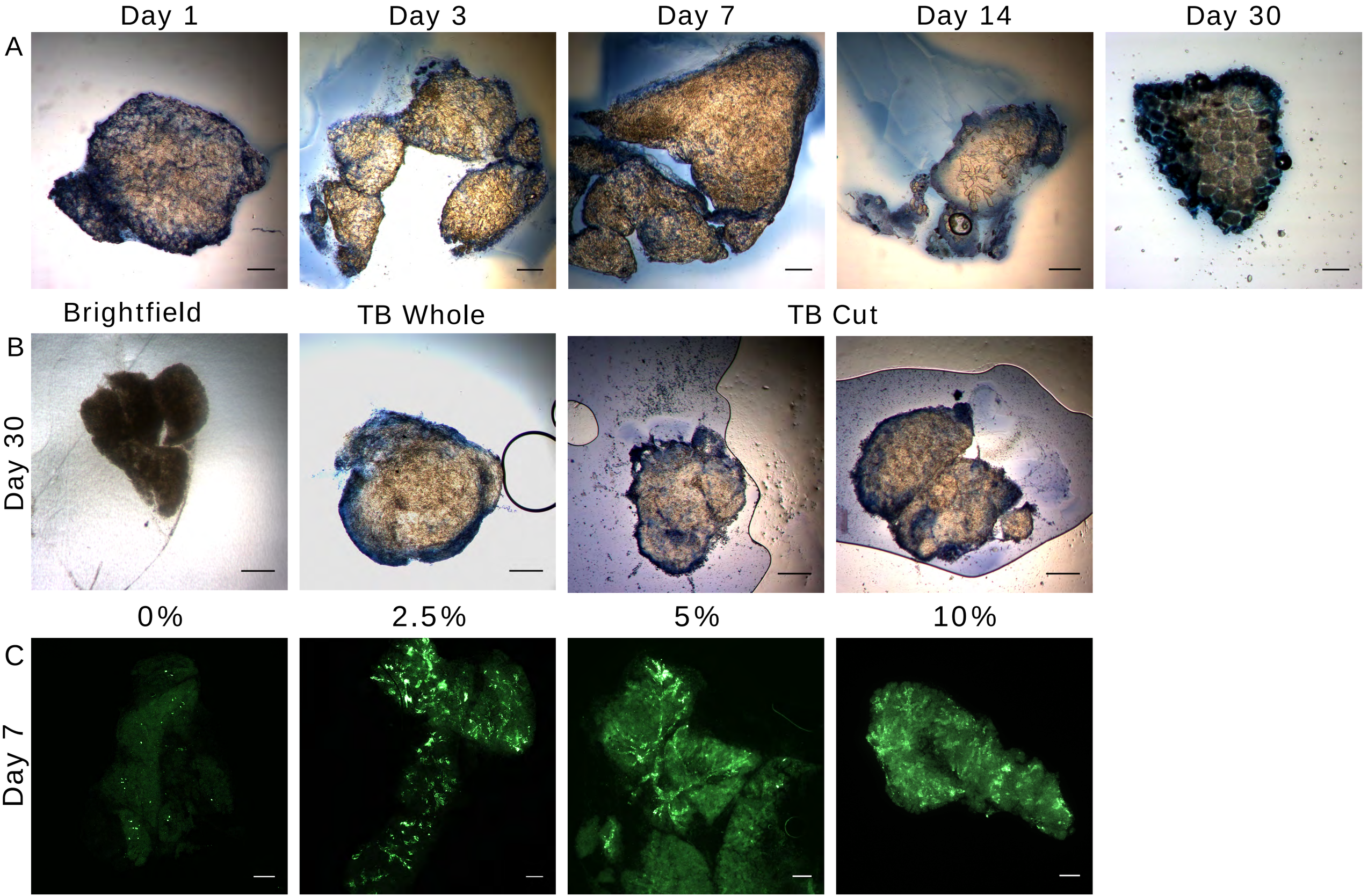

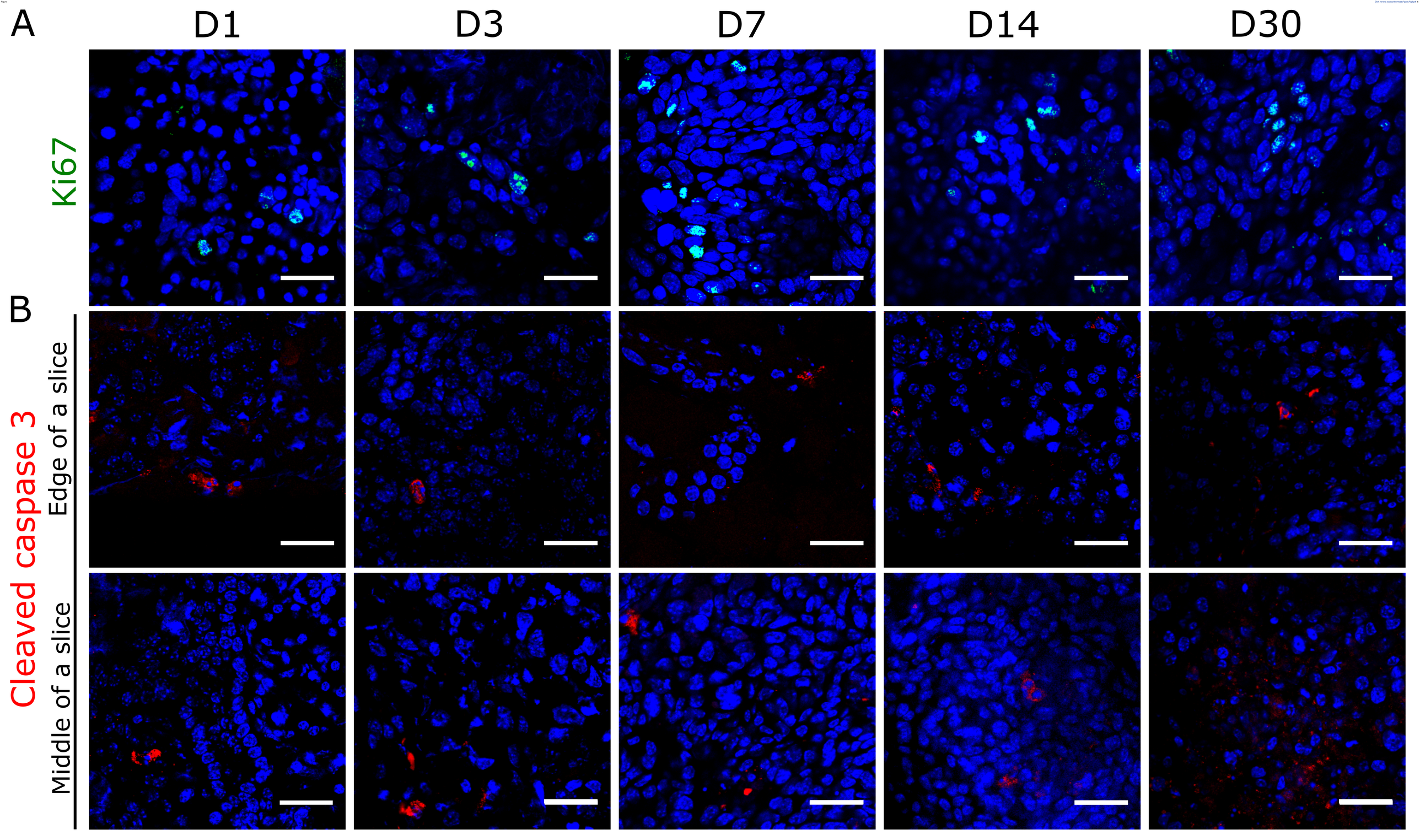

A

D1

D7

D14

D30

E-cadherin

SMA

Phalloidin

B

D1

D3

D7

D14

CD31

TUBB3

Aqp5

A

D1

D3

D7

D14

Ki67

B

Amylase

d

C

Aqp5

D

E-cadherin

E

TUBB3

F

CD31

Untreated

Irradiated

D8

D2

D4

D8

A

Ki67

B

Cleaved Caspase3

C

Phalloidin

D

Amylase

E

E-cadherin

Untreated

Irradiated

D8

D2

D4

D8

A

Ki67

B

Cleaved Caspase3

C

Phalloidin

D

Aqp5

E

E-cadherin

Figure

Table of Materials

Click here to access/download;Table of Materials;JoVE_Materials (feb edits).xls

Name of Material/ Equipment	Company	Catalog Number	Comments/Description
Vibratome VT1000S	Leica Biosystems	N/A	Vibratome for sectioning
Double Edge Stainless Steel Razor Blades	Electron Microscopy Sciences	72000	
Agarose	Fisher Scientific	BP165-25	Low-melt
Parafilm	Sigma-Aldrich	P6543	
Penicillin-Streptomycin-Amphotericin B	Lonza	17-745H	PSA
24-well plate	CellTreat	229124	
Dulbecco's Phosphate Buffered Saline (DPBS)	Gibco	14190-144	
Loctite UltraGel Control Superglue	Loctite	N/A	Purchased at hardware store
Natural Red Sable Round Paintbrush	Princeton Art & Brush Co	7400R-2	
Gentamicin Sulfate	Fisher Scientific	ICN1676045	
Transferrin	Sigma-Aldrich	T-8158-100mg	
L-glutatmine	Gibco	25030-081	
Trace Elements	MP Biomedicals	ICN1676549	
Insulin	Fisher Scientific	12585014	
Epidermal Growth Factor	Corning	354001	
Hydrocortisone	Sigma-Aldrich	H0888	
Retinoic acid	Fisher Scientific	R2625-50MG	
Fetal Bovine Serum	Gibco	A3160602	
DMEM/F12 Media	Corning	150-90-CV	
Millicell Cell Culture Insert	Millipore Sigma	PICM01250	12 mm, 0.4 um pore size for 24 well plate
0.4% Trypan Blue	Sigma-Aldrich	T8154	
LIVE/DEAD Cell Imaging Kit (488/570)	Thermo-Fisher	R37601	Only used LIVE dye component
Anti-Ki-67 Antibody	Cell Signaling Technology	9129S	
Anti-E-cadherin Antibody	Cell Signaling Technology	3195S	
Anti-Cleaved Caspase-3 Antibody	Cell Signaling Technology	9661L	
Anti-SMA Antibody	Sigma-Aldrich	C6198	
Anti-amylase Antibody	Sigma-Aldrich	A8273	
Anti-CD31 Antibody	Abcam	ab28364	
Anti-TUBB3 Antibody	Cell Signaling Technology	5568S	
Alexa Fluor 594 Antibody Labeling Kit	Thermo-Fisher	A20185	
Alexa Fluor 594 Phalloidin	Thermo-Fisher	A12381	
Bovine Serum Albumin	Fisher Scientific	BP1600	
Triton X-100	Sigma-Aldrich	21568-2500	
Paraformaldehyde Prills	Fisher Scientific	5027632	
New England Nuclear Blocking Agent	Perkin Elmer	2346249	No longer sold
DAPI	Cell Signaling Technology	4083S	
Prolong Gold Antifade Mounting Media	Invitrogen	P36934	
Leica SPSII Spectral Confocal	Leica Biosystems	N/A	For confocal imaging
Leica DMIL Inverted Phase Contrast Microscope	Leica Biosystems	N/A	
Cobalt-60 Teletherapy Instrument	Atomic Energy of Canada Ltd Theratron-80	N/A	
Amac Box, Clear	The Container Store	60140	Agarose block mold

1 Alewife Center #200
Cambridge, MA 02140
tel. 617.945.9051
www.jove.com

ARTICLE AND VIDEO LICENSE AGREEMENT

Title of Article:	Radiation Treatment of Organotypic cultures from submandibular and parotid salivary glands models key in vivo characteristics
Author(s):	Rachel Meyer, Wen Yu Wong, Roberto Guzman, Randy Burd, Kirsten Limesand

Item 1: The Author elects to have the Materials be made available (as described at http://www.jove.com/publish) via:

☉ Standard Access ☐ Open Access

Item 2: Please select one of the following items:

☉ The Author is **NOT** a United States government employee.

☐ The Author is a United States government employee and the Materials were prepared in the course of his or her duties as a United States government employee.

☐ The Author is a United States government employee but the Materials were NOT prepared in the course of his or her duties as a United States government employee.

ARTICLE AND VIDEO LICENSE AGREEMENT

1. **Defined Terms.** As used in this Article and Video License Agreement, the following terms shall have the following meanings: "**Agreement**" means this Article and Video License Agreement; "**Article**" means the article specified on the last page of this Agreement, including any associated materials such as texts, figures, tables, artwork, abstracts, or summaries contained therein; "**Author**" means the author who is a signatory to this Agreement; "**Collective Work**" means a work, such as a periodical issue, anthology or encyclopedia, in which the Materials in their entirety in unmodified form, along with a number of other contributions, constituting separate and independent works in themselves, are assembled into a collective whole; "**CRC License**" means the Creative Commons AttributionNon Commercial-No Derivs 3.0 Unported Agreement, the terms and conditions of which can be found at: http://creativecommons.org/licenses/by-ncnd/3.0/legalcode; "**Derivative Work**" means a work based upon the Materials or upon the Materials and other preexisting works, such as a translation, musical arrangement, dramatization, fictionalization, motion picture version, sound recording, art reproduction, abridgment, condensation, or any other form in which the Materials may be recast, transformed, or adapted; "**Institution**" means the institution, listed on the last page of this Agreement, by which the Author was employed at the time of the creation of the Materials; "**JoVE**" means MyJove Corporation, a Massachusetts corporation and the publisher of The Journal of Visualized Experiments; "**Materials**" means the Article and / or the Video; "**Parties**" means the Author and JoVE; "**Video**" means any video(s) made by the Author, alone or in conjunction with any other parties, or by JoVE or its affiliates or agents, individually or in collaboration with the Author or any other parties, incorporating all or any portion of the Article, and in which the Author may or may not appear.

2. **Background.** The Author, who is the author of the Article, in order to ensure the dissemination and protection of the Article, desires to have the JoVE publish the Article and create and transmit videos based on the Article. In furtherance of such goals, the Parties desire to memorialize in this Agreement the respective rights of each Party in and to the Article and the Video.

3. **Grant of Rights in Article.** In consideration of JoVE agreeing to publish the Article, the Author hereby grants to JoVE, subject to **Sections 4** and **7** below, the exclusive, royalty-free, perpetual (for the full term of copyright in the Article, including any extensions thereto) license (a) to publish, reproduce, distribute, display and store the Article in all forms, formats and media whether now known or hereafter developed (including without limitation in print, digital and electronic form) throughout the world, (b) to translate the Article into other languages, create adaptations, summaries or extracts of the Article or other Derivative Works (including, without limitation, the Video) or Collective Works based on all or any portion of the Article

1. / 1 Alewife Center #200 / Cambridge, MA 02140

jove

ARTICLE AND VIDEO LICENSE AGREEMENT

discretion, elect not take any action with respect to the Article until such time as it has received complete, executed Article and Video License Agreements from each such author. JoVE reserves the right, in its absolute and sole discretion and without giving any reason therefore, to accept or decline any work submitted to JoVE. JoVE and its employees, agents and independent contractors shall have full, unfettered access to the facilities of the Author or of the Author's institution as necessary to make the Video, whether actually published or not. JoVE has sole discretion as to the method of making and publishing the Materials, including, without limitation, to all decisions regarding editing, lighting, filming, timing of publication, if any, length, quality, content and the like.

12. **Indemnification.** The Author agrees to indemnify JoVE and/or its successors and assigns from and against any and all claims, costs, and expenses, including attorney's fees, arising out of any breach of any warranty or other representations contained herein. The Author further agrees to indemnify and hold harmless JoVE from and against any and all claims, costs, and expenses, including attorney's fees, resulting from the breach by the Author of any representation or warranty contained herein or from allegations or instances of violation of intellectual property rights, damage to the Author's or the Author's institution's facilities, fraud, libel, defamation, research, equipment, experiments, property damage, personal injury, violations of institutional, laboratory, hospital, ethical, human and animal treatment, privacy or other rules, regulations, laws, procedures or guidelines, liabilities and other losses or damages related in any way to the submission of work to JoVE, making of videos by JoVE, or publication in JoVE or elsewhere by JoVE. The Author shall be responsible for, and shall hold JoVE harmless from, damages caused by lack of sterilization, lack of cleanliness or by contamination due to the making of a video by JoVE its employees, agents or independent contractors. All sterilization, cleanliness or decontamination procedures shall be solely the responsibility of the Author and shall be undertaken at the Author's expense. All indemnifications provided herein shall include JoVE's attorney's fees and costs related to said losses or damages. Such indemnification and holding harmless shall include such losses or damages incurred by, or in connection with, acts or omissions of JoVE, its employees, agents or independent contractors.

13. **Fees.** To cover the cost incurred for publication, JoVE must receive payment before production and publication of the Materials. Payment is due in 21 days of invoice. Should the Materials not be published due to an editorial or production decision, these funds will be returned to the Author. Withdrawal by the Author of any submitted Materials after final peer review approval will result in a US$1,200 fee to cover pre-production expenses incurred by JoVE. If payment is not received by the completion of filming, production and publication of the Materials will be suspended until payment is received.

14. **Transfer, Governing Law.** This Agreement may be assigned by JoVE and shall inure to the benefits of any of JoVE's successors and assignees. This Agreement shall be governed and construed by the internal laws of the Commonwealth of Massachusetts without giving effect to any conflict of law provision thereunder. This Agreement may be executed in counterparts, each of which shall be deemed an original, but all of which together shall be deemed to me one and the same agreement. A signed copy of this Agreement delivered by facsimile, e-mail or other means of electronic transmission shall be deemed to have the same legal effect as delivery of an original signed copy of this Agreement.

A signed copy of this document must be sent with all new submissions. Only one Agreement is required per submission.

CORRESPONDING AUTHOR

Name:	Kirsten Limesand
Department:	Nutritional Sciences
Institution:	University of Arizona
Title:	Professor
Signature:	[signature]
Date:	11/19/12

Please submit a **signed** and **dated** copy of this license by one of the following three methods:

1. Upload an electronic version on the JoVE submission site
2. Fax the document to +1.866.381.2236
3. Mail the document to JoVE / Attn: JoVE Editorial / 1 Alewife Center #200 / Cambridge, MA 02140

Responses to Reviewers' Comments on manuscript EMID: e334840c2d49e554

We thank the editor and reviewers for their constructive analyses and thoughtful suggestions. Point-by-point responses to the specific issues are provided below:

Response to Editor:

1. *Please take this opportunity to thoroughly proofread the manuscript to ensure that there are no spelling or grammar issues.* We have proofread the manuscript for spelling and grammar issues.
2. *Please obtain explicit copyright permission to reuse any figures from a previous publication. Explicit permission can be expressed in the form of a letter from the editor or a link to the editorial policy that allows re-prints. Please upload this information as a .doc or .docx file to your Editorial Manager account. The Figure must be cited appropriately in the Figure Legend, i.e. "This figure has been modified from [citation]."* We thank the editor for this recommendation. All the figures in this manuscript are original and have not been previously published.
3. *Please define all abbreviations before use, e.g., PBS, FBS, etc.* All abbreviations have been defined as recommended.
4. *Please use h, min, s for time units.* All time units have been edited as recommended.
5. *Step 5.3: What's the temperature for incubation?* The incubation temperature has been added to Step 5.2.2 in the revised version.
6. *7.3: Is it Colbalt-60 or Cobalt 60?* Cobalt-60 is the proper nomenclature and has been consistently used in the updated manuscript.
7. *Please do not abbreviate journal titles for all references.* All the references have been edited according to the new instructions.
8. *There is a 2.75 page limit for filmable content. Please highlight 2.75 pages or less of the Protocol steps in yellow (including headings and spacing) for filming that identifies the essential steps of the protocol for the video, i.e., the steps that should be visualized to tell the most cohesive story of the Protocol.* We have highlighted sections for potential filmable content.

Response to Editor: Comments from 2/1

1. *Please take this opportunity to thoroughly proofread the manuscript to ensure that there are no spelling or grammar issues.* The manuscript has been proofread for grammar and spelling mistakes.
2. *JoVE cannot publish manuscripts containing commercial language. This includes company names of an instrument or reagent. Please remove all commercial language from your manuscript and use generic terms instead. All commercial products should be sufficiently referenced in the Table of Materials and Reagents. Examples of commercial language in your manuscript include* Commercial language has been removed from lines 108, 109, 112, 115, 155, 171, 203, 213, 231, 285, and 326.
3. *Please do not highlight notes for filming.* Notes have been excluded from highlighted text in lines 131, 132, 167, 168, 284, and 285.

4. *Please specify all antibodies in the manuscript.* Antibodies have been specified in lines 295, 311, and 316.
5. *Please use µL instead of µl.* µl has been replaced with µL in lines 181, 191, 198, 199, 227, 254, 295, 314, and 334.
6. *Please remove trademark (™) and registered (®) symbols from the Table of Equipment and Materials.* Trademark symbols have been removed from the Table of Materials.

Response to Reviewer 1:

Questions:

Intro: In second paragraph of Introduction, it's worthwhile to specify 2D cell culture, rather than cell culture in general. Some groups culture salivary-derived cells in 3D either on or within scaffolds. We have edited the introduction to clarify the culture system of prior research (lines 58-62).

1. *Protocol 1.3. Should "paraffin" be "parafilm"?* The text has been modified to exclude all commercial language according to editor comment #2 from 2/1.
2. *Protocol 2.3. Add 1.5 mL or 1.0 mL, respectively, *per well*, correct?* In the edited manuscript, we have added this detail in line 160.
3. *Protocol 3.3. Was this meant to say "a 12 mm diameter, 0.4 µm pore size …" rather than 30mm? Only the 12 mm insert seems to be listed in Materials.* All data within the figures were conducted on 12mm diameter inserts and the text has been updated accordingly (lines 174-176).
4. *Protocol 3.3. When the salivary section is laid on the membrane insert, is it expected that the 300 µL of media would reach the membrane bottom? i.e. should the tissue also be in contact with media? It's probably worthwhile to specify this for readers, as they'll likely be wondering prior to using the method.* We have edited the text to clarify this process in lines 174-176.
5. *Protocol 4. This is unclear - it seems to be making the same FBS-containing media as is already described in 3.2, and then culturing "in FBS conditions" which is already described. Please explain and/or revise.* This section has been deleted as recommended.
6. *Protocol 6.4 "permeabilization"* We have edited the text accordingly (lines 250-253).
7. *Protocol 6.9. and 6.12. Can you estimate a volume to use for these two steps?* We have provided an approximate volume for both of these steps (lines 262-263, 273-275).
8. *Protocol 6.18 Can you estimate a volume to use here? Also, it's probably worthwhile to note that bubbles are very easily acquired with ProLong, and advise on how to minimize this, as it can interfere with imaging.* We have provided more details about this process in lines 293-295.
9. *Protocol 6.18. and 7. The introduction of section 7 seems to be the details of the mounting for section 6.18. Please move this "NOTE" over to section 6.18 (as 6.18.1, etc.), as these details really are important for mounting with ProLong.* We moved the text per the recommendation.
10. *Protocol 7. Section 7 feels either redundant/unnecessary, or very underdeveloped. I suggest that it is moved out to section 6, or further developed in Protocol 7 with more details - i.e. what is important for the confocal imaging? I'd say that recommendations on magnification/objective (4x? 10x? 20x?), and corresponding Nyquist settings for optical section thickness are really key. Stitching the z-stacks together is probably also desirable, and tips here would also be good to share.* We have provided more details on how to image the slices using confocal microscopy.

11. *Protocol 8. (7.3, 7.4) This is a typo; subsections should be 8.1 and 8.2. But it seems that much more detail is warranted here, as the radiation treatment is really the key difference for this entire protocol. How should sample be arranged, in relation to irradiator? What distance from source? What kind of irradiator? (in Materials) How long is a typical exposure? Is it acceptable to irradiate the tissue *before* sectioning?* We have provided more details on how to irradiate the samples and moved the irradiation protocol to section 4. We have not addressed whether or not the tissue can be irradiated prior to sectioning.
12. *I do not see a protocol for phalloidin staining. Please add this.* We have provided a note about phalloidin staining (269-271).
13. *Figure 1: It is unclear what the conclusion is from the experiment in Figure 1. Which condition was best? How was that determined from the brightfield images?* Data from both Figure 1 and 2 were utilized to assess culture conditions. Optimal culturing conditions was based on observations using phase contrast on an inverted microscope with cells appearing bright and retractile as viable and increasing cellular darkness as dying, nonviable organ cultures. This was confirmed through assessments of tissue area stained positive for Trypan blue and the amount of cells incorporating the live cell stain.
14. *Figure 2: What %FBS was used in the culture in Figure 2? I did not see this information listed in the Figure caption. And, while trypan blue's typical use is evident, it is difficult to determine what the data in Fig 2A is showing. i.e. How is the conclusion for Fig 2 ("We visually observe high number of Trypan blue positive cells in 0% FBS culture conditions while higher FBS culturing conditions exhibit fewer blue positive cells (Figure 2A and 2B).") supported by those Figure panels?* We have added details about FBS conditions across all the figures. We have also included more text on the observations and conclusion from Figure 2 (lines 331-353).
15. *Figure 3: What FBS level was used for this culture?* We used 2.5% FBS in Figure 3 and have edited the figure legend accordingly.
16. *Figure 3A: Ki67 staining should be nuclear, and although patterns can vary, the images in D14 do not look like positive Ki67, as there is no overlap with nuclei. Images in D14 also appear to be processed differently, as the small amount of overlapping channels do not appear as a bright cyan color (i.e. for tightly overlapping blue and green signals). For a method-based manuscript like this one, this D14 data isn't optimal for demonstrating a trend. Can the authors revise this?* We have repeated the Ki67 staining and presented representative images.
17. *Figure 3B: Cleaved Caspase: The authors don't resolve how cleaved caspase staining is seemingly low in these images, but peripheral trypan blue staining is so high, especially at late timepoints. These two assessments (demonstrating cell death) should be related, correct?* These two assessments do not implicitly measure the same thing; Trypan blue measures viability on unfixed tissues and cleaved caspase-3 specifically measures apoptosis in fixed tissues. Cleaved caspase-3 images were taken in central sections of the tissue and correspondingly there is little trypan blue staining in these areas. We have also presented cleaved caspase-3 images of the tissue edges, which does not recapitulate the peripheral Trypan blue staining.

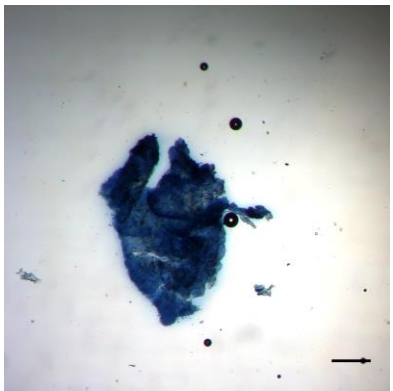

The high peripheral trypan blue staining noted by the reviewer is a small % of the total area of the cultured section. The image to the left represents a truly dead section and the peripheral Trypan blue color is much darker than a majority of images presented in Figure 2.

18. *Figure 5: Why are sections stained again for Ki67? If this signal isn't overlapped directly with alpha-amylase, then it seems redundant here.* Figure 5 is from parotid sections and Figure 3 is from submandibular sections, so these are distinct analyses.
19. *Figure 6: A key hallmark of radiotherapy (RT)-induced xerostomia is a loss of acinar cell populations, and a replacement with immune infiltrate, adipose, scar, or other repair/remodeling cells and ECM. Here, the authors do not use these indicators (e.g. by staining for alpha-amylase positive acinar cells over time); instead, the success of their RT model hinges on the disruption of actin filaments at a single timepoint, day 8.*
There are a number of radiation-induced cellular changes in the salivary gland that have been reported in the literature including, reductions in amylase, apoptosis of acinar cells, compensatory proliferation of acinar cells, loss of polarity and disruptions in cytoskeletal structure. In addition, there are acute and chronic hallmarks of RT and the ones noted in this comment are all chronic phenotypes. Therefore, the intent of the analysis of irradiated vibratome cultures was to evaluate many of these phenotypes as feasible. Apoptosis of parotid acinar cells is observed in D2 (24 hrs after IR) and apoptosis in submandibular acinar cells is observed at D2 and D4 (24 and 72 hrs after IR), which is similar to previously reported *in vivo* analysis. Parotid and submandibular vibratome cultures have increases in proliferation at D8 (7 days after IR), which is similar to previously reported *in vivo* analysis. As noted by the reviewer, the cytoskeletal changes are similar to our most recent report on radiation damage to salivary glands. We have added analysis of acinar cell markers in Figures 6 and 7. As for immune infiltrates, the cultures were irradiated *ex vivo* so this would not be feasible analysis. In addition, the adipose and fibrotic (scar) changes are at much later time points in the literature (>30 days); therefore the vibratome culture methodology would not be able to address these outcomes.

Although the authors are recognized as deeply involved in the field, this criterion for evaluating the model seems like a somewhat generic mechanism, and isn't convincing without (a) more references to other published data that reinforce the proposed success criteria, and (b) a complementary non-radiated control tissue at day 8. The control tissue in Fig 7 was stained at D1. Unfortunately, the D8 RT-treated section resembles a staining artifact that can occur commonly with phalloidin in 3D treatment (i.e. loss of signal in the last sample in a bunch). The D1 untreated represented the tissue architecture at the time of radiation and later time points in culture were presented in Figure 4. We have revised the radiation figures to the reviewer's suggestion. As noted in the previous response, we evaluated a number of cellular changes in irradiated vibratome cultures to demonstrate the feasibility of this methodology.

20. *Please add to Materials list: - Parafilm (and probably capitalize, as it is a trade name), Embedding molds, Irradiator.* These have been added as recommended.

Responses to Reviewer #2:

1. *More details on the irradiation should be provided. Which irradiator (model, and cat no) Are the samples uncovered during this step? What is the duration of the treatment?* We have provided more details about how the irradiation process should be performed in section 4 of the protocol.
2. *It seems logical to put the irradiator treatment before the fixation and processing of the samples rather than after the whole process.* We have moved the irradiator treatment section as requested.
3. *The brightfield an ICC images show clear and continuous loss of tissue integrity throughout the course of the experiment that conflicts with many of the authors interpretations. Fig.3. The lack of progressive increase in the SMG cleaved caspase 3 signal indicates that the accumulation of this marker of intrinsic pathway apoptosis is either transient and not an accurate indicator of apoptosis, or that the cells are dying by a caspase 3-independent apoptosis pathway, or through another mechanism, such as necrosis. Since the Ki67 levels also do not change, this figure does not reflect the progressive cell loss and this marker does not seem particularly useful except maybe to rule out cell cycle entry and proliferation. The authors should remove this figure or combine with other markers discussed below to indicate that the system is not valid beyond perhaps 14 days.* We respectfully disagree that there is a continuous loss of tissue integrity. We respectfully disagree with these conclusions. The brightfield images depict some shrinkage of the cells; however, this is likely a volume effect rather than a loss of tissue integrity because E-cadherin levels remain high and located at the plasma membrane. In addition, the overall tissue viability remains high as determined by minimal central trypan blue staining, low levels of cleaved caspase-3 and high levels of staining using the live cell dye. The levels of cleaved caspase-3, Ki-67 and live cell stain are similar to Su et al who evaluated human vibratome sections. None of these indicators suggest that there is a progressive cell loss. We do concur with the assessment that the day 30 cultures have some deteriorations from earlier time points and we have transparently shown this to the readers to allow them to make their own assessments on how to use this methodology.
4. *Fig. 4. The markers in 4A show a striking loss of SMG tissue structure after day 14, particularly in the loss of membrane localized E-cadherin, suggestive that most E-cadherin expression beyond day 14 is in dead cells or cells that have likely undergone EMT. This conclusion is consistent with the SMA and phalloidin profiles. In 4B, the loss of Aqp5 at day 7 indicates that functional studies of the gland slices are only valid through day 7, and that functional studies that require innervation or vasculature may not be valid after day 3.* The difficulty in observing E-cadherin noted by the reviewer appears to be based on the yellow color used to present the images. We have changed this to red and the membrane staining is much more apparent. As noted above, E-cadherin staining is maintained for the entire 30-day culture period. We have noted in the results the markers that are maintained acutely versus those that are sustained longer.

5. *Fig. 5. The amylase stains suggest that PG functional studies may be valid only through day 7.* Due to the smaller size of the parotid gland, we obtained fewer sections and did not have sample to evaluate at later time points. We have added further analysis to demonstrate that amylase positive cells are readily detectable at day 14 albeit it is reduced compared to the earlier time points. Even if the reviewer is correct and the PG is only functional through day 7, this is significantly longer than the previously published study of 48 hours.
6. *Fig. 6. The comparison of day 1 untreated with days 2, 4, and 8 after irradiation (and the markers chosen) precludes meaningful conclusions of the ability of the slice cultures to be used to model gland irradiation. This figure and conclusions about the effects of irradiation should be removed or the authors should acknowledge that the data indicate irradiation causes a loss of tissue structure without any insight into mechanisms, which does not seem useful enough to merit inclusion. Alternatively, the data could be reworked to show E-cadherin and Aqp5/Amy in parallel irradiated samples. However, based on the literature, these studies may require intact vasculature and/or innervation which may limit the ability of the slice cultures to model longer term irradiation damage and which should also be addressed.* The D1 untreated represented the tissue architecture at the time of radiation and later time points in culture were presented in the untreated cultures in Figure 4. There are a number of radiation-induced cellular changes in the salivary gland that have been reported in the literature including, reductions in amylase, apoptosis of acinar cells, compensatory proliferation of acinar cells, loss of polarity and disruptions in cytoskeletal structure. Therefore, the intent of the analysis of irradiated vibratome cultures was to evaluate many of these phenotypes. Apoptosis of parotid acinar cells is observed in D2 (24 hrs after IR) and apoptosis in submandibular acinar cells is observed at D2 and D4 (24 and 72 hrs after IR), which is similar to previously reported in vivo analysis. Parotid and submandibular vibratome cultures have increases in proliferation at D8 (7 days after IR), which is similar to previously reported in vivo analysis. Cytoskeletal changes in parotid and submandibular vibratome sections are observed at D8 (7 days after IR) and are similar to our most recent report on radiation damage to salivary glands. We have modified the untreated images to day 8 in culture as recommended and added E-cadherin, Aqp5 and amylase images. Notably, new data for the parotid gland in figure 5 suggests that the vascular and neuronal structures are maintained better than in the submandibular gland. As for mechanisms, this recommendation is outside the scope of the instructions of this methods journal.
7. *Details of the vibratome (company, model number) should be provided in the text.* The vibratome details are included in the Table of Materials; however, editor comment #2 from 2/1 prevents us from including these details in the manuscript.
8. *More detail regarding the specs on the paintbrush should be provided.* We have included these details in the Table of Materials.
9. *Should other publications be referenced for the culture media or is this the first publication using it?* Media was based off of our 2D primary culture media with the exception of FBS concentration and the addition of pen-strep.
10. *The authors should explain why two 1X PBS washes are needed with each media change. Typically, less disruption to 3D cultures is preferred. Presumably, if used, the PBS should be sterile*

and prewarmed, which should be mentioned. The finalized culturing method no longer includes a media change; therefore, this has been deleted.

11. *Is the storage after Step 6.3 in PBS or PBT? The time frame for storage should be indicated.* The original text of PBS for the storage is correct. Time frame has been updated in text (lines 244-246).
12. *Step 6.7. Define NEN*. NEN is a trademark name used by PerkinElmer and it stands for New England Nuclear; this detail has been added to the Table of Materials.
13. *Step 6.12 Is incubation for 1.5 hrs really sufficient for this step?* We observe positive staining in the center of our vibratome sections, which suggests that it is a sufficient amount of time for the secondary antibody incubation. Of note, both previously published studies on vibratome sections from salivary glands utilized a one hour incubation.
14. *Step 7. Sealing of coverslips with nail polish should be mentioned as required for long-term storage.* This information can be found in step 6.18.2.
15. *Its not clear why PG were not stained for AQP5. Is this channel protein maintained longer in the PG slice cultures?* These images have been added to Figure 5.
16. *Fig.2. Trypan blue staining can indicate panoramic changes in viability, as observed around the tissue slice edges, but is not suitable for assessing single cell or multicellular tissue compartment viability. The authors should provide an alternative method with improved sensitivity for monitoring viable cells, such as live cell staining kits that detect active esterases or acknowledge this limitation in the text.* We have added a live cell stain to Figure 2.
17. *Fig. 5. The absence of PG CD31 and tubb3 stains for endothelial cells and nerves, respectively, makes the validity of functional studies that require either vasculature or innervation not possible, and the authors should acknowledge this limitation.* We have acknowledged this limitation in the discussion (lines 377-383).
18. *Reference 14 is incorrect for Su et al. https://www.ncbi.nlm.nih.gov/pubmed/27214128*. We edited this reference accordingly.

Responses to Reviewer #3:

1. *There should be more discussion/commentary on the importance of the culture media and FBS gradients in the vibratome culture media (3.2 on page 3 of 12). A rationale for testing different FBS concentrations and the final recommended FBS level would be appreciated.* We have added more rationale to the FBS experiment and clarified the recommendation (lines 327-331, 350-353).
2. *A demonstration/discussion showing the transfer of the culture plates/dishes between the biology laboratory and the radiation facility and placing the cultures in the radiation machine would be helpful for viewers who are interested in using the system to study the effect of radiation on SGs.* Additional information regarding radiation has been added in protocol section 4.
3. *Please spell out "NEN" blocking agent.* NEN is a trademark name used by PerkinElmer and it stands for New England Nuclear; this detail has been added to the Table of Materials.
4. *It is interesting that the trypan blue data appear to show more dead cells on the surface than in the center of the organotypic cultures. A comment on this observation would be helpful for the*

viewers. We have added more data and discussion on this observation in the revised manuscript.

5. *The authors may want to comment/speculate on whether or not the PG organotypic cultures would be expected to remain viable with functional capacity for up to 30 days and if not why?* We have added more parotid time points and the tissue architecture appears to be maintained better than the submandibular gland. That said, it is likely to deteriorate between days 14 and 30 similar to the submandibular gland.